

## MRI acoustic noise reduction using CNN

DOI : 10.36909/jer.17661

Mohamed H. Al-Meer \*

Department of Computer Science Engineering, College of Engineering, Qatar University

\* Corresponding Author: almeer@qu.edu.qa

### ABSTRACT

Presented in this paper is a revolutionary deep learning-based architecture for reducing the noise generated during Magnetic Resonance Imaging (MRI) scans. The proposed architecture differs from the usual adaptive algorithms used in Active Noise Control (ANC). In the present work, we are exploring the use of Deep Convolutional Artificial Networks to recognize advanced sounds. By applying the DL-NN to a 513-time segment, a 180-degree phase shift sample of the noise is generated. After computational simulation analyses were performed, experimental results show that performance in noise average power can be reduced by approximately 10 to 15 dB.

**Keywords:** Deep Learning, CNN, ANC, MRI Acoustic Noise, Noise Cancellation, Noise Reduction.

### INTRODUCTION

An MRI is an extremely effective medical tool used to diagnose a wide range of medical problems, but it is accompanied by noises whenever it is operated. These noises are unpleasant and cause hearing loss when they are repeatedly used.

The MRI machine's acoustic noise has been well known since its invention as a source of unbearable noise. This noise caused discomfort for both the patient as well as the nearby staff (More et al., 2006, Counter et al., 1997, Wang 2017, Moelker et al., 2003) MRI noise is produced by ten different pulsed radiofrequency waves transmitted from the gradient coils in

large MRI scanners employed for clinical imaging. As a result, high-intensity acoustic noise is generated. Acoustic noise accounts for most of the Sound Pressure Levels (SPLs) caused by MRI acoustic contribution. As part of the MRI process, machines proceed through a series of stages, including magnetization-prepared rapid gradient echo, fast gradient echo turbo, and spin-echo T1/2 mm, among others. The noise generated by those stages can reach up to 117 decibels. Among the different modulation strategies used, the rapid pulse rate modulation strategy, amplitude-modulated pulse envelopes, and multi-peaked spectra have the largest contribution to SPL.

In order to suppress MRI noise levels, passive solutions, such as sound absorbers, are used; however, this method has two disadvantages: the first is its low reduction effect, the second is that it is relatively effective for low frequencies only.

There are numerous active methods that can be employed to reduce the noise exposure to the patient and to those present in the MRI scanning room (but not to eliminate it completely). Research has incorporated active noise control techniques (ANC) commonly used for sound noise suppression (Rudd et al., 2013, Liu et al., 2011, Rudd et al., 2012, Li et al., 2008, Takkar et al., 2017, Kannan et al., 2010, Jung et al., 2005, Ramachandran et al., 2010) ANC was widely used in the MRI to reduce noise, but only targeted the patient and was worn via headsets.

In 1936, (Lueg, P., 1936) proposed and tested the ANC basic idea. He used a microphone to measure a sound wave and added this to a 180-degree phase-shifted anti-signal to the main one by using a speaker. Taking their analysis into account, promising results have been obtained. To suppress noise, the controller unit outputs an anti-noise signal, which is added to the base noise by a second path, which creates a destructive interference effect and reduces noise significantly. How the algorithm generates the anti-noise signal is the secret of the algorithm. In Figure 1, the concept of using a secondary signal for noise cancellation is shown.

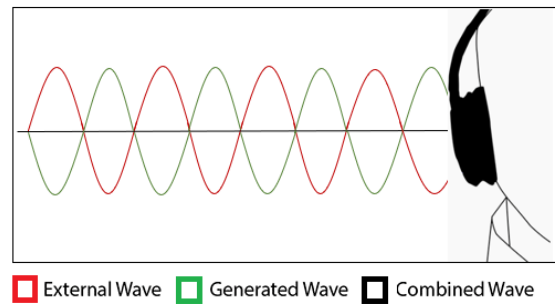


**Figure 1.** Formation of noise, anti-noise, and residual signals in an ANC system

As part of noise suppression, adaptive digital filters consisting of Finite Impulse Response (FIR) and Infinite Impulse Response (IIR) filters are used (Lu et al., 2021). Although they achieved good suppression of narrow-band and low-band noises, they did not achieve satisfactory suppression of broad-band noises. Furthermore, the FIR and IIR filters need continuous adjustment and pre-knowledge of the microphone, speaker, and path transfer functions in order to generate the anti-noise signal correctly.

There have been many studies examining the use of neural networks (NN) to cancel noise and improve speech quality (Zhang et al., 2021, Lee et al., 2021, Park et al., 2016). There is evidence that it improves speech recognition in noisy environments, while raising the signal-to-noise ratio of sound signals.

Today's ANC systems use MRI-compatible microphones and headphones that the patient wears in conjunction with an error microphone. Patients wear the headphones to reduce noise passively as well as to provide some entertainment while the scanner works. As a patient, he is protected from noise by a passive system, whereas any listener in the room may perceive the environment as noisy. It is important to reduce that noise for both the patient and the guest in the room without causing any complications. In almost all research, this scheme has been used to target patients lying on their backs, however in this study, we plan to target an individual who is seated in a specific place. In this method, we use an ANN model that uses deep learning to quantify noise reduction with minimum hardware requirements. In comparison with regular ANC, it reduces a lot of hardware components.

In his paper (Goldman et al., 1989), Goldman discusses the earliest implementation of ANC in MRI noise suppression. His team tried feeding a synthesized MRI sound wave with the opposite phase to a recorded MRI sound wave, but they did not achieve good results. The author of (Mechefske et al., 2002) tested a pneumatic tube to deliver noise cancelling sounds to a headset. Ultimately, the tube-based system was less effective in achieving a satisfactory reduction effect due to the large delay caused by the length of the tube.

In (Pla et al., 1995), piezoelectric speakers near the person's ears were used with an adaptive algorithm called FXLMS, in ANC, the most popular adaptive algorithm is the filtered-x least-mean-square algorithm. According to the report, the noise reduction was acceptable across a frequency range of 0 Hz to 1500 Hz. A feedback controller using cascaded NN was tested by (Mcjury et al., 1997) and (Chen et al., 1999) utilizing recorded MRI noise and a speaker. They performed the experiment in the lab and found some promising results.

There is another implementation of feedforward MRI ANC that uses piezoelectric speakers driven by optical signals (Kahana et al., 2004). The claimed results were a reduction in MRI SPL of between 35 - 50 dB. In (Li et al., 2008), a group of researchers used a feedback controller to suppress an EPI sequence, reported to be the loudest MRI sound. Other work has focused on other MRI sequences, such as the GEMS (Chen et al., 1999) and EPI (Rudd et al., 2009). Those works reported a considerable reduction in noise power, but the reduction was only effective below 2000 Hz.

Besides deep learning, Artificial neural networks (ANN) have been used recently to solve the problem of noise reduction inside MRI scanning rooms (Chen et al., 2010, Salamsi et al., 2011, Chang et al., 2009). This study aims to provide a quiet zone within the MRI room for an accompanying person and even for the patient himself without using any passive attenuators. The headsets can both be taken off, allowing the loud sound to be partially isolated and normal life patterns to resume. The solution will be based on both deep learning and FFT for spectrum content learning.

Specifically, the following sections of the paper will be presented: Section II will illustrate the basics of ANC using FIR filtering, Section III will cover the proposal for deep learning in more detail. The experimental setups and the results in section IV are explained, section V will present the discussion and future works, while, the conclusion in section V is presented.

### ACTIVE NOISE CANCELLATION

An example of a simple ANC model can be seen in Figure 1. It is ANC's principle that, when we add an audio wave with its inverse, the resulting waveform will be cancelled. In addition to noise and anti-noise waveforms, the system uses two measurement microphones. First, we have a reference microphone that records the noise at the source. Next, we have an error microphone that records the noise created. The location is close to where we need it to be quiet (away from noise).

Input to the ANC adaptive unit is residual noise  $e(t)$  recorded by the error microphone. By processing this signal,  $y(t)$ , the canceling signal, is generated. As illustrated in Figure 2, the ANC system uses  $d(n)$  to denote the source of noise at the microphone's neighboring position.  $W(z)$  accepts  $e(n)$  the error signal and generates  $y(n)$ , which controls the loudspeaker  $S(z)$ . The loudspeaker and its secondary path transfer function are included in  $S(z)$ .

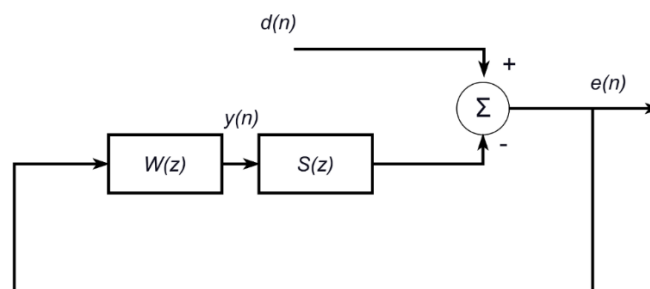


**Figure 2.** A block diagram of a feedback ANC system

ANC can be classified into two types: feed-forward controls and feedback controls. In the first type, the cancellation signal is taken from an original noise source, and the anti-noise

signals are placed in the noise propagation path, which produces the quiet zone. In Figure 3.A, an example of feedforward active noise cancellation in action is shown. A single microphone is used in the feedback control to determine the residual or error noise that should be reduced and used in generating the cancelling signal, as shown in Figure 3B.

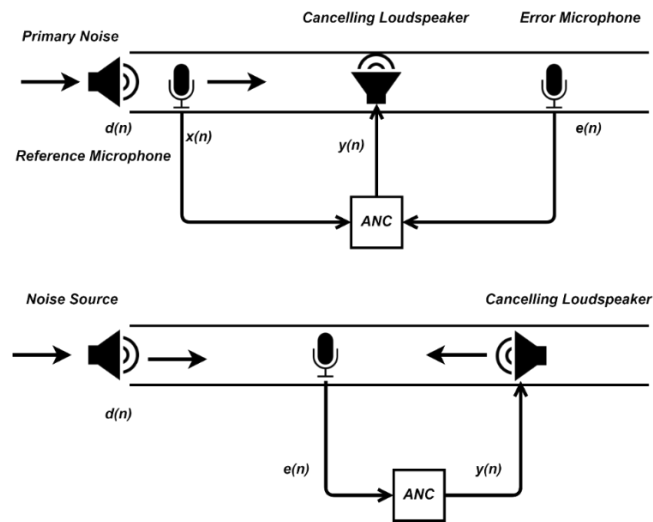


**Figure 3.** (Upper Figure) ANC systems utilize feedforward technology to cancel noise.

(Bottom Figure) This system is known as the feedback ANC system.

Adaptive weight is an effective method of determining the primary path. Following the adaptation, the filter will learn the filter weights and provide a digital representation of the filter. Least-Mean-Square algorithm (LMS) or one of its variants is the most widely known algorithm for updating filter weights. Figure 2 shows the secondary path between speaker and microphone that must be considered. There is a secondary path (feedback path) that connects the anti-noise speaker to the noise reference microphone, which needs to be subtracted. The residual noise signal or error signal  $e(n)$  is shown in Figure 4. The adaptive unit processes  $e(n)$  to generate the cancelling signal  $y(n)$ . The adaptive weights are represented by  $W(z)$ , and the secondary path transfer function is  $S(z)$ . We only consider time-invariant linear transfer functions. In addition, we will assume both the microphones and the speaker are ideal for this study.

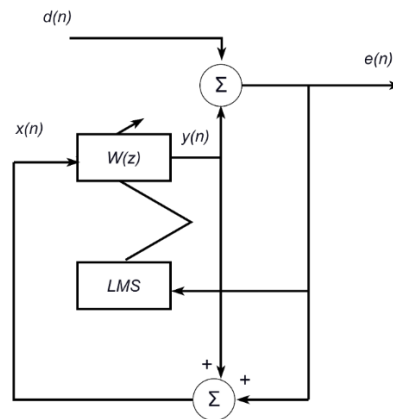


**Figure 4.** Adaptive ANC system using the LMS algorithm.

We propose to replace the filter weights  $W(z)$  with Deep CNNs based on deep learning adaptive learning. The replacement is illustrated in Figure 5. Additionally, there will be a microphone located near the source of noise  $d(n)$ , as well as a speaker located near the quiet area. While the input training sound file should be recorded in the source zone, the target noise sound should be recorded near the quiet zone.

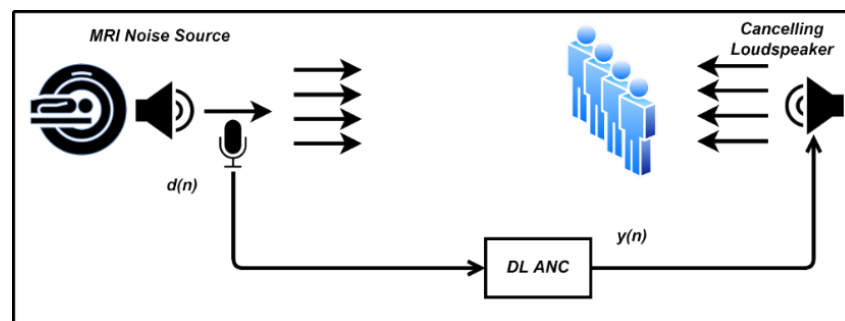


**Figure 5.** Block diagram of predictor using NN

## DATASET PREPARATION & FEATURES TRANSFORMATION

Using the model presented previously, we propose a Deep Learning solution for MRI sound suppression. The data set was downloaded from (Kaska, et al., 2021), which helped in preparing the training set. It contains several recordings of three types of MR sequences, namely EPI, EPI, MDEFT and GEMS.

At 44.1 kHz, the audio signal was recorded for 33 minutes, 34 seconds. To compute the

spectral vector block, we use a Hamming Window of 512 samples and a 1024-point Short Time Fourier Transform (STFT) with a 50% overlap. For each frequency bin, the frequency resolution was 43.06 Hz (44.1kHz/1024). By dropping the frequency symmetric half corresponding to negative frequencies, the spectral vector was reduced to 513 units. Input features of the predictor are constructed from the MRI STFT magnitude vector (size 513 X 1, duration 23.2 ms). The predictor input feature format for the DL model consists of 20 consecutive MRI STFT magnitude vectors (size 513 X 20, duration 232 ms). Based on the current STFT vector and the 19 previous noisy STFT vectors, the STFT output estimate is computed.

To achieve unit variance and zero mean, the predictor and target vectors were both normalized and standardized. This model is shown in Figure 6. In order to convert the target signal to the time domain, we use the magnitude spectrum and the phase of the predictor signal.

### **DEEP LEARNING MODEL STRUCTURE**

We will use the same known model for speech denoising that proved proficiency, with the 2D CNN deep architecture (Shah, A., 2019). There is no special model that suits Deep Learning Active Noise Control (DL-ANC), but the speech denoising model fits MRI sound suppression goal perfectly. Based on the results of the tests, in addition to other studies, we have come to this conclusion.

Deep learning is a very complex regressive learning model consisting of multiple layers of NN. The breakthrough in DL was the development of a revolutionary learning algorithm (error backpropagation algorithm) that can learn multi-layered NN with many layers. The most commonly used deep learning model is CNN (Convolutional Neural Network), and we propose a model that uses deep learning to reduce MRI noise instead of a conventional adaptive filter.

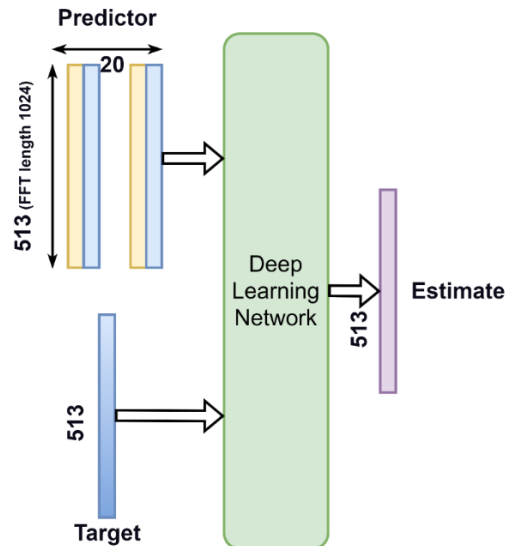


**Figure 6.** The arrangement of features for training and inference in a deep learning network

It starts with a convolution layer with 15 convolutional filters each of size 15 by 15, the second layer is a drop-off by one, followed by a pooling layer with a pool size of 3 by 3, then a second convolutional layer of size 5 by 5, followed by a drop-off, pooling layer of 3 by 3, and a stride of 2. Layer 4 has a convolutional layer of number 10 with 3 2 by 2 filter sizes. This is followed by a dropout layer, followed by a max pooling layer of number 3 with a pooling size of 2 by 2 and a stride of 1. After a flattened layer, we have a dense layer of 800 units with Relu activation function, preceded by another dense layer of 513 units. The total training blocks reached 188,815 blocks.

### TRAINING & TESTING SETUP

A sample of one of the MRI noise sounds is shown in Figure 7 showing three different MRI sequences. The differences are obvious, but all share the loudness property by displaying the waveform of a 100,000-point MR noise signal, figure 8 illustrates how effectively the ANC system works. By adding the corresponding anti-noise signal generated by the proposed ANC system to the source sound, the residual signal waveform is produced as depicted in Figure 8.

As seen in Figure 9, the spectrum is plotted for the MRI noise. Blue plots depict source MRI

noise spectrum, and red plots depict operated-on MRI noise spectrum (residual waveforms after noise reduction) or can be called control-on and control-off MRI spectrums, respectively. We can see in this spectrum figure that the MR noise energy is primarily present at low frequencies (from 0 to 3 KHz), while the ANC system has been very effective at reducing noise. A 10-15 dB drop in SPL power can be observed in this area. The two waveforms possess similar power levels after the 3 KHz bandwidth, which shows that this would be effective for a specific low-frequency bandwidth.

To have even more deeper performance evaluation for the controller, the method performance is evaluated in terms Normalized Mean Square Error (NMSE). We can define NMSE as shown in equation 1.

$$NMSE = 10 \log_{10} \frac{\sum_{n=1}^L e(n)^2}{\sum_{n=1}^L d(n)^2} \quad (1)$$

The residual error signal is measured as  $e(n)$ , while the baseline MRI noise is measured as  $d(n)$ . Furthermore, The NMSE value is usually below zero, and always lower values reflect better noise attenuation. Table 1 shows the performance of the DNN-ANC control. The computed values were extracted from a random 100,000 samples. It demonstrates that the control reduces the MRI noise signal. The Table contains rows for the overall SPL power, the overall reduction power, the average reduction power for each consecutive 1000 samples in the sequence, the maximum reduction power, besides the maximum reduction frequency.

**Table 1.** Simulation results typical measurements.

<b>Features</b>	<b>Uncontrolled</b>	<b>DNN-ANC Controlled</b>
Overall SPL power	34.06 dB	27.36 dB
Overall reduction power (NMSE)	N.A.	-6.71 dB
Average NMSE reduction power	N.A.	-6.70 dB
Maximum reduction power	N.A.	12 dB
Maximum reduction frequency	N.A.	1200 Hz

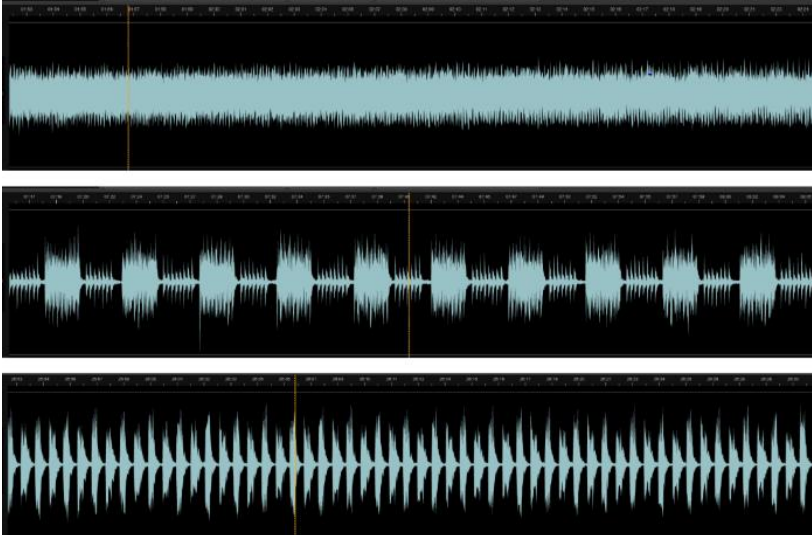


**Figure 7.** Comparisons between source MRI noise responses for three different scan types.

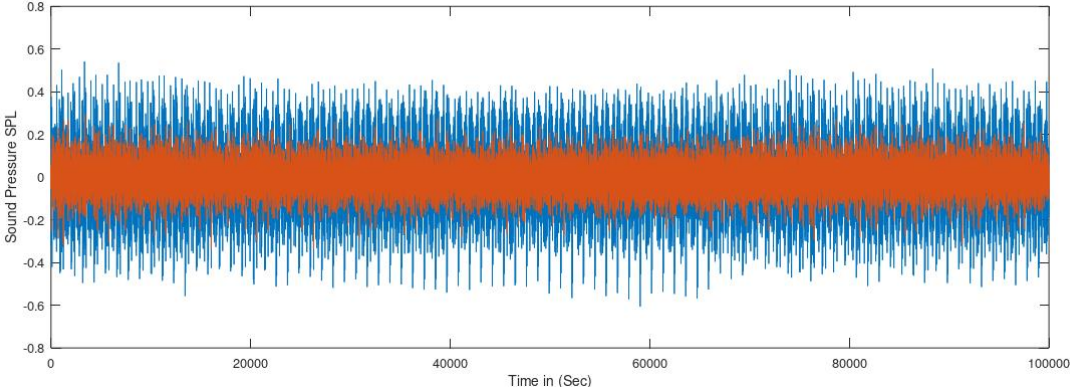


**Figure 8.** Sample waveform of the acoustic source noise generated by a MR imager (100K samples) in blue and the residual (error) signal waveform in red.

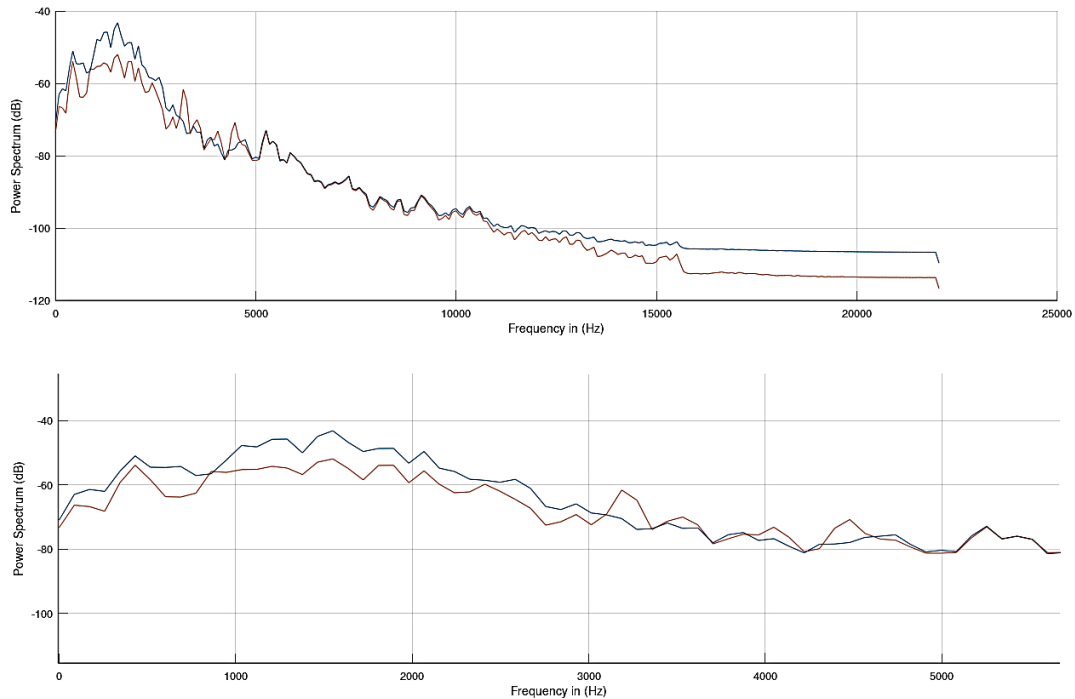


**Figure 9.** Spectrum of the MRI noise. Spectrum of untreated MRI noise (red line) treated MRI acoustic signal after applying feedback control (blue line). The upper graph is for bandwidth up to  $SR/2 = 22$  KHz, and the lower plot is an expanded bandwidth of  $[0, 5$  KHz].

## DISCUSSION AND FUTURE WORK

An offline simulation of 3-T MR Scanner acoustic reduction has been implemented while working on EPI, MDEFT and GEMS sequences. A CNN-dependent Deep Learning strategy was used to form the recognition sequence to produce the correct anti-noise sequence to reduce the noise coming from the primary path. As far as the author's knowledge is concerned, this study is the first to employ DL to reduce MR acoustic noise. Therefore, many references do not support comparisons. However, some are listed below, although having different similarities.

For example, the next table, Table 2, shows some of the works related to MRI acoustic noise suppression, but mostly using one of the ANC methods, it was taken for comparison

purposes. The five related studies mentioned will use ANC with a variant of the LMS method to achieve reasonable simulated noise suppression. Noise reduction ranged from 10 dB to 30 dB, but these results were obtained for specific frequency ranges and principal components. EPI and Pulsed EPI was the main MRI sequence test chosen because of its high disturbance effect, but we have taken even two other sequences, namely MDEFT and GEMS sequences, which showed similar noise reduction effects as seen in the EPI sequence.

**Table 2.** Average MRI acoustic power reduction for other works.

Reference	Methods	MRI Sequence	Noise Reduction (dB)
[Mcjry, M. et al., 2021]	General ANC Feed-Forward XLMS	Gradients and Pulse sequences	30 dB (0 - 700 Hz)
[Kannan, G. et al., 2011]	feedback ANC	EPI	17-20 dB
[Rudd, B. et al., 2012]	FXLMS ANC	EPI	10.6 dBA across audible spectrum
[Li, M. et al., 2008]	ANC [feedback, feedforward, hybrid]	EPI and EPI Pulse sequences	20 dB over principal frequency component
[Li, M. et al., 2009]	Tailored FXLMS	EPI and EPI Pulse sequences	principal harmonic up to 12 dB
Current study	Deep NN (CNN)	3 MRI sequences	6.7 dB in average

The results should guide future work towards the actual implementation of the proposed technology beyond simulation. In addition, another future expectation will be to use in-room responses (transfer function) alongside speakers' non-linearities to further adapt to better responses.

Other work has mentioned that [Zhang, H., et al., 2021], typical ANC methods have shown minimal results when handling nonlinearities of speakers and high-frequency components in suppressed noise. However, when DL used general noise suppression, it produced stronger reduction effects. This was the basis for the use of DL in active sound suppression. Thus, on the basis of this fact, we assume that future work will surely be expected to take into consideration the speaker that generates the anti-noise non-linearity in addition to the scanner room transfer function.

Though our study gave a respectful reduction of noise in dB, it was perceptible. It can be seen as an encouragement to continue work which needs to be modified in order to achieve comparable reduction effects in future studies.

## CONCLUSION

An approach that utilizes deep learning is described in this paper to address the problem of MRI Noise reduction. When deep ANC is used, the loudest noises are selectively cancelled in the 3 KHz bandwidth where they are more likely to occur. Systematic evaluations demonstrate the effectiveness and robustness of using a deep NN ANC to attenuate MRI noise in noisy scanning rooms. As a result of this successful demonstration, we look forward to further work on DNN-based autoencoder as well as other types of NN, such as the LSTM, and besides Recurrent Neural Networks (RNNs), to provide better noise reduction.

## REFERENCES

- Chang, C. Y. 2009.** Simple approaches to improve the performance of noise cancellation. *Journal of Vibration and Control*, 15(12), 1875-1883.
- Chen, C. K., Chiueh, T. D., & Chen, J. H. 1999.** Active cancellation system of acoustic noise in MR imaging. *IEEE transactions on biomedical engineering*, 46(2), 186-191.
- Counter, S. A., Olofsson, A., Grahn, H. F., & Borg, E. 1997.** MRI acoustic noise: sound pressure and frequency analysis. *Journal of Magnetic Resonance Imaging*, 7(3), 606-611.
- Goldman, A. M., Gossman, W. E., & Friedlander, P. C. 1989.** Reduction of sound levels with antinnoise in MR imaging. *Radiology*, 173(2), 549-550.
- Jung, K. J., Prasad, P., Qin, Y., & Anderson, J. R. 2005.** Extraction of overt verbal response from the acoustic noise in a functional magnetic resonance imaging scan by use of segmented active noise cancellation. *Magnetic Resonance in Medicine: An Official Journal of the International Society for Magnetic Resonance in Medicine*, 53(3), 739-744.

**Kahana, Y., Kots, A., Mican, S., Chambers, J., & Bullock, D. 2004.** Opto-acoustical ear defenders with active noise reduction in an MRI communication system. In INTER-NOISE and NOISE-CON Congress and Conference Proceedings (Vol. 2004, No. 9, pp. 1009-1024). Institute of Noise Control Engineering.

**Kannan, G., Milani, A. A., Panahi, I. M., & Briggs, R. W. 2010.** An efficient feedback active noise control algorithm based on reduced-order linear predictive modeling of fMRI acoustic noise. *IEEE transactions on Biomedical Engineering*, 58(12), 3303-3309.

**Kaska Erim, 2021.** A variety of typical MRI-generated acoustic sounds. Accessed November 15, 2021. Available from: <https://www.youtube.com/watch?v=6Aj2QspPf7s>.

**Lee, H. 2021.** Noise reduction system by using CNN deep learning model. *Indonesian Journal of Electrical Engineering and Informatics (IJEEI)*, 9(1), 84-90.

**Li, M., Lim, T. C., & Lee, J. H. 2008.** Simulation study on active noise control for a 4-T MRI scanner. *Magnetic resonance imaging*, 26(3), 393-400.

**Li, M., Rudd, B., Lim, T. C., & Lee, J. H. 2011.** In situ active control of noise in a 4 T MRI scanner. *Journal of Magnetic Resonance Imaging*, 34(3), 662-669.

**Lu, L., Yin, K. L., de Lamare, R. C., Zheng, Z., Yu, Y., Yang, X., & Chen, B. 2021.** A survey on active noise control techniques--Part I: Linear systems. *arXiv preprint arXiv:2110.00531*.

**Lueg, P. 1936.** Process of silencing sound oscillations. US patent 2043416.

**McJury, M., Stewart, R. W., Crawford, D., & Toma, E. 1997.** The use of active noise control (ANC) to reduce acoustic noise generated during MRI scanning: some initial results. *Magnetic resonance imaging*, 15(3), 319-322.

**Mechefske, C. K., Geris, R., Gati, J. S., & Rutt, B. K. 2001.** Acoustic noise reduction in a 4 T MRI scanner. *Magnetic Resonance Materials in Physics, Biology and Medicine*, 13(3), 172-176.

**Moelker, A., & Pattynama, P. M. 2003.** Acoustic noise concerns in functional magnetic resonance imaging. *Human brain mapping*, 20(3), 123-141.

**More, S. R., Lim, T. C., Li, M., Holland, C. K., Boyce, S. E., & Lee, J. H. 2006.** Acoustic noise characteristics of a 4 Telsa MRI scanner. *Journal of Magnetic Resonance Imaging: An Official Journal of the International Society for Magnetic Resonance in Medicine*, 23(3), 388-397.

**Park, S. R., & Lee, J. 2016.** A fully convolutional neural network for speech enhancement. arXiv preprint arXiv:1609.07132.

**Pla, F. G. 1995.** Active control of noise in magnetic resonance imaging. *Active 95*, 573-583.

**Ramachandran, V. R., Panahi, I. M., & Milani, A. A. 2010.** Objective and subjective evaluation of adaptive speech enhancement methods for functional MRI. *Journal of Magnetic Resonance Imaging*, 31(1), 46-55.

**Rudd, B. W., Lim, T. C., Li, M., & Lee, J. H. 2012.** In situ active noise cancellation applied to magnetic resonance imaging. *Journal of vibration and acoustics*, 134(1).

**Rudd, B. W., Lim, T. C., Lee, J. H., & Li, M. 2013.** Evaluation of MRI compatible headphones for active noise control. *Noise Control Engineering Journal*, 61(1), 41-49.

**Rudd, Brent W., et al. 2012.** In situ active noise cancellation applied to magnetic resonance imaging. 011017.

**Salmasi, M., Mahdavi-Nasab, H., & Pourghassem, H. 2011.** Comparison of feed-forward and recurrent neural networks in active cancellation of sound noise. In *2011 International Conference on Multimedia and Signal Processing (Vol. 2, pp. 25-29)*. IEEE.

**Shah, Arpit, 2019.** Accessed November 15, 2021, available from: <https://github.com/dwtcourses/Speech-Denoising-using-DNN-CNN-and-RNN>

**Takkar, M. S., Sharma, M. K., & Pal, R. 2017.** A review on evolution of acoustic noise

reduction in MRI. In 2017 Recent Developments in Control, Automation & Power Engineering (RDCAPE) (pp. 235-240). IEEE.

**Wang, Y. 2017.** Gradient coil design and acoustic noise control in magnetic resonance imaging systems.

**Zhang, H., & Wang, D. 2021.** Deep ANC: A deep learning approach to active noise control. Neural Networks, 141, 1-10.